Quaternary International 243 (2011) 16–32

Contents lists available at ScienceDirect

Quaternary International

journal homepage: www.elsevier.com/locate/quaint

A stratigraphic framework for the Pliocene–Pleistocene continental sediments of the Guadix Basin (Betic Cordillera, S. Spain)

S. Pla-Pueyo [a,*], C. Viseras [a], J.M. Soria [b], José E. Tent-Manclús [b], A. Arribas [c]

[a] Dpto. Estratigrafía y Paleontología, Facultad de Ciencias, Campus Fuentenueva, Universidad de Granada. 18071 Granada, Spain
[b] Dpto. Ciencias de la Tierra y del Medio Ambiente, Facultad de Ciencias, UA. Apdo. Correos 99. 03080 Alicante, Spain
[c] Área de Investigación en Patrimonio Geológico. Dpto. Investigación en Recursos Geológicos, Instituto Geológico y Minero de España. 28003 Madrid, Spain

ARTICLE INFO

Article history:
Available online 1 February 2011

ABSTRACT

The central sector of the Guadix Basin (Betic Cordillera, S. Spain) hosts some of the most significant Pleistocene large-mammal sites in Europe. The basin infill is divided into six genetic units, the three lower with marine sediments and the remainder mainly continental. As the environmental characterization of the sediments is crucial to understand the ecologic and geologic processes leading to the formation of these sites, a stratigraphic, sedimentologic and petrologic study is presented. Combining a lithologic correlation with previous biostratigraphic data and new magnetostratigraphic data, a detailed litho-, bio- and magnetostratigraphic scheme has been developed for the study area. It shows the stratigraphic architecture of the central sector of the Guadix Basin, together with the age and the relative spatial position of the most important mammal sites. As well, it has been also helpful to identify several isochronous surfaces, to establish the exact position and the age of the boundary between the two last units of the continental infill in the Guadix Basin and to calculate sedimentation rates.

1. Introduction

The Guadix and Baza Basins (Betic Cordillera, S. Spain) are part of the Neogene–Quaternary Guadix-Baza Depression, in which a number of paleontologic sites from the central sector of the Guadix Basin has been discovered since 2000 in conjunction with the Fonelas Project (Viseras et al., 2006; Arribas et al., 2009; Web page of the Fonelas Project). Despite extensive research on the stratigraphy and sedimentology of the Guadix Basin, most of it developed from several Ph.D. dissertations (Peña, 1979; Viseras, 1991; Soria, 1993; García-Aguilar, 1997; García-García, 2003; Pla-Pueyo, 2009, among others) and the publications derived from them (e.g. Viseras and Fernández, 1992; 1994; 1995; Soria et al., 1998, 1999; García-García et al., 2006a,b; 2009; Pla-Pueyo et al., 2007; 2009a,b,c), a more detailed stratigraphic architecture scheme was developed following the recent finding of 47 Pleistocene large-mammal sites.

This paper presents results from part of a multidisciplinary study focused on the central sector of the Guadix Basin, where most of the abovementioned sites appear. The study combines litho-, bio-, and magnetostratigraphic techniques because of the difficulty in correlating some of the measured stratigraphic profiles by standard methods and the lack of a numerical age for the paleontologic sites. The time-control provided by magnetostratigraphy enhanced the ability to date events during the formation of the basin, to calculate sedimentation rates as well as to establish the influence of allogenic processes. Use of paleomagnetic measurements has been successfully used to date vertebrate sites all over the world (MacFadden et al., 1983; Biquand et al., 1990; Zijderveld et al., 1991; Whitelaw, 1992; Opdyke et al., 1997; Corvinus and Rimal, 2001; Napoleone et al., 2003; Dennell et al., 2006; Barnosky et al., 2007; Wang et al., 2007; Boehme et al., 2009; among others). A well-established magnetostratigraphic framework serves to guide and constrain interpretations about mammal evolution and intercontinental dispersal of land mammals (Lindsay, 2001). Magnetostratigraphic data of the Pliocene and Pleistocene vertebrate sites located in the Baza Basin sediments exists (Oms et al., 1994, 1999; Agustí et al., 1997, 1999, 2001a,b; Garcés et al., 1997), but this paper presents paleomagnetic data from the neighboring Guadix Basin for the first time within an integrated stratigraphic scheme for the central sector of the Guadix Basin.

* Corresponding author.
E-mail addresses: sila.pla@gmail.com (S. Pla-Pueyo), viseras@ugr.es (C. Viseras), jesus.soria@ua.es (J.M. Soria), je.tent@ua.es (J.E. Tent-Manclús), a.arribas@igme.es (A. Arribas).

1040-6182/$ – see front matter © 2011 Elsevier Ltd and INQUA. All rights reserved.
doi:10.1016/j.quaint.2011.01.028

With the establishment of several isochronous surfaces, the age of the contact between the last genetic units of the infill of the Guadix Basin, together with the ages of the main paleontologic sites, are refined, allowing the calculation of sedimentation rates during the evolution of the basin during the last 3.8 Ma.

2. Regional setting

The Betic Cordillera is located on the southern Iberian Peninsula (Fig. 1A) and represents the most western belt of the Alpine Orogen. The Guadix Basin (Fig. 1B) is situated in the central sector of the Betic Cordillera, within Granada Province (Spain). It seals the ancient contact between the two main structural realms of the Betic Cordillera: the Internal Zones (or Alboran Block) (Andrieux et al., 1971) and the External Zones (corresponding to the folded and faulted South Iberian paleomargin) (Viseras et al., 2005).

As well as in other Neogene intramontane basins in the Betic Cordillera, two main sedimentary stages have been identified in the Guadix Basin during its evolution (Viseras et al., 2005). The older stage, Late Tortonian in age, is marine, while the younger is continental, lasting from the Late Tortonian to the Late Pleistocene (Fernández et al., 1996a; Viseras et al., 2005). There are several proposed models in the literature for the whole Guadix-Baza Depression, such as the one by García-Aguilar and Martín (2000) based mainly in the lacustrine sediments. However, the predominant fluvial style of the Guadix Basin sediments led to the decision to divide the continental stage into six genetic units (Fig. 2), following the model by Fernández et al. (1996a). Units I and II correspond to the marine sedimentation stage, while Unit III

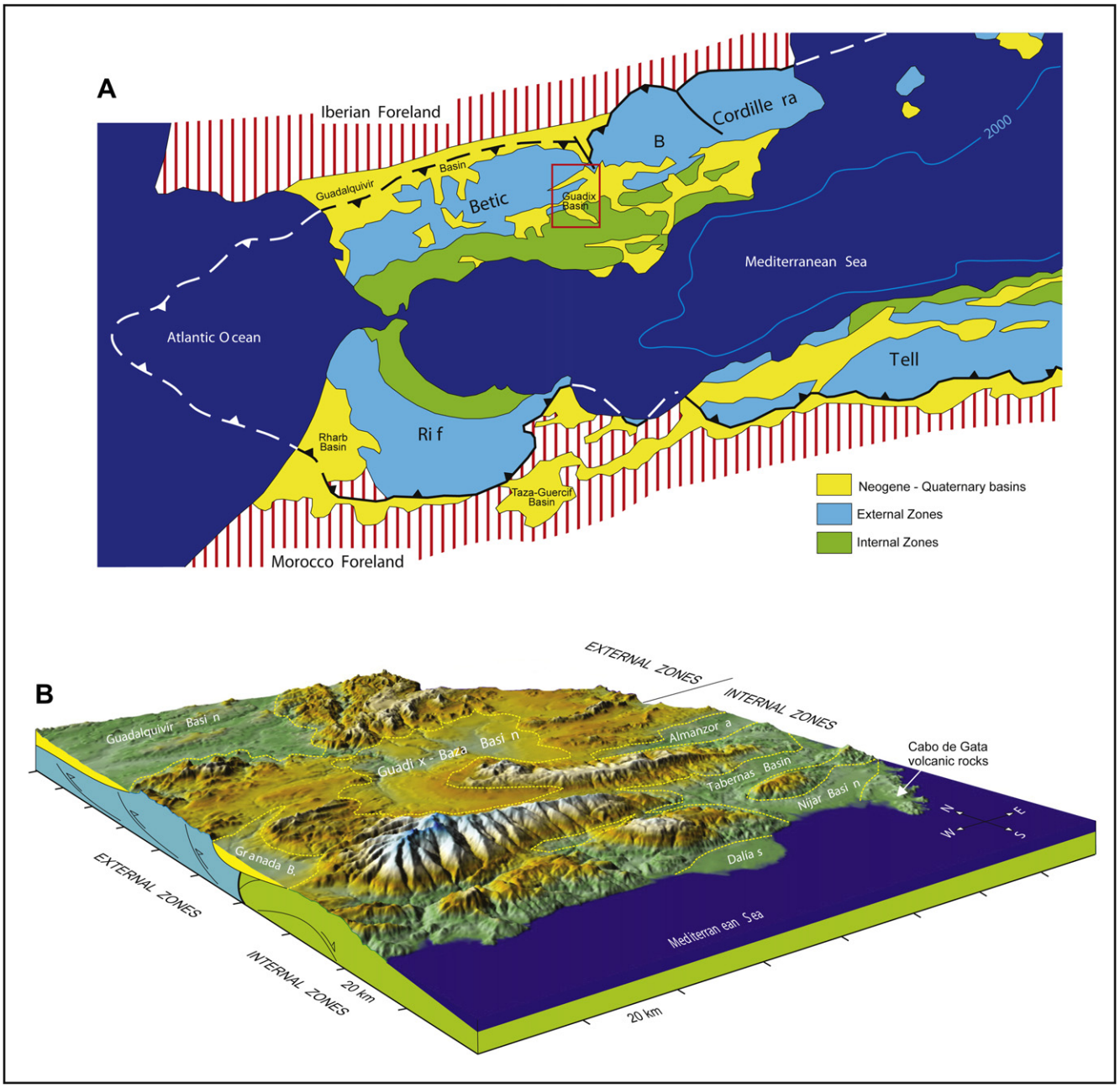

Fig. 1. A. Geologic map of the Betic Cordillera, showing the position of the Guadix Basin. The rectangle represents the study area. B. Geologic context of the Guadix Basin.

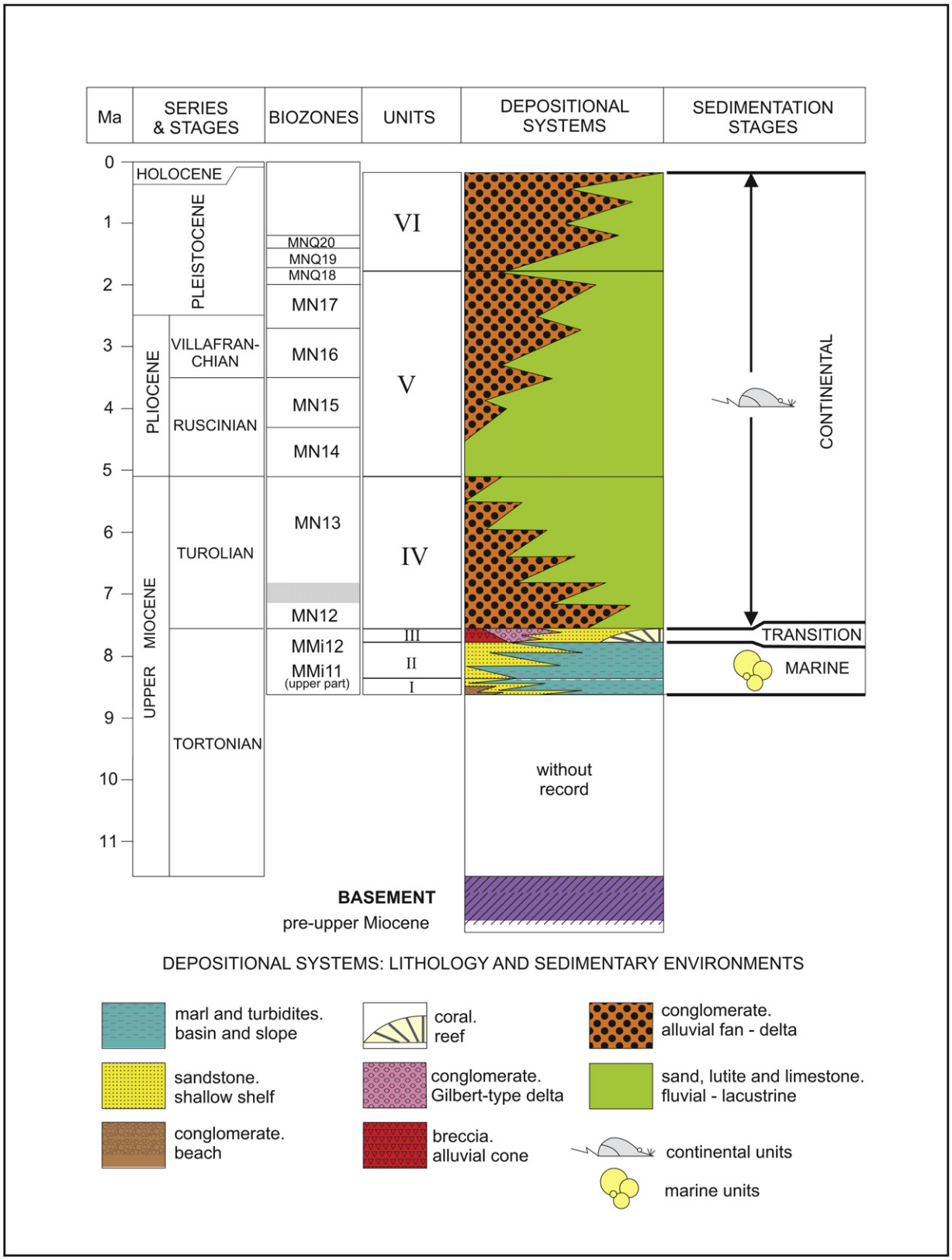

Fig. 2. Genetic units of the infill of the Guadix Basin (modified from Fernández et al., 1996a).

contains shallow marine sediments, deposited through the latest Tortonian sea withdrawal from the central sector of the Betic Cordillera. The continental stage of infilling (Late Tortonian–Late Pleistocene) corresponds to the three youngest units (IV, V and VI). During this stage, the basin drained into the neighboring Baza Basin, reaching its final filling stage in the Late Pleistocene (top of Unit VI), when a stream piracy process triggered the change of the basin from endoreic to exoreic, enhancing the erosion of the basin infill to the present (Viseras and Fernández, 1992; Calvache et al., 1996; Fernández et al., 1996b; Calvache and Viseras, 1997; Soria et al., 1998, 1999).

Only sediments belonging to units V and VI crop out in the central sector of the Guadix Basin. Within these two units, three main drainage systems can be distinguished (Fernández et al., 1996b; Viseras et al., 2006) (Fig. 3). The so-called Axial System flowed parallel to the paleogeographic axis of the basin, toward the NE. This fluvial-lacustrine longitudinal drainage system drained into a large shallow lake, located to the East in the neighboring Baza Basin, which acted as base level for the whole depression. The Axial System (AS) was fed by two transverse alluvial systems. The Internal Transverse System (ITS) (Viseras and Fernández, 1994, 1995) had large coalescent alluvial fans forming a "bajada" system, with their source area located on the Internal Zones of the Betic Cordillera. On the other hand, the External Transverse System (ETS) (Fernández et al., 1991, 1993), which received its inputs from the erosion of the External Zones of the Betic Cordillera, was composed of small isolated alluvial fans and fan deltas.

The present study is focused on the fluvial-lacustrine deposits of the Axial valley (AS), as they host a number of important macromammal fossil sites in units V and VI (Pliocene and Pleistocene) (Viseras et al., 2006; Arribas et al., 2009).

3. Materials and methods

3.1. Lithostratigraphy and correlations

Several stratigraphic profiles were measured in the central sector of the Guadix Basin, collecting lithologic, sedimentologic and paleontologic data. Using photomosaics, geometry and sequences were identified. Architectural elements (Miall, 1978, 1985; 1996) were recognized in 2D and 3D where possible, establishing hierarchic relationships between them, and a lithofacies code, based in previous classifications (Miall, 1978, 1985, 1996; Viseras et al., 2006, 2009; Pla-Pueyo et al., 2007; 2009a,c), has been established. Lithostratigraphic correlation is based mainly on field observations (bed to bed correlation and geologic mapping).

3.2. Magnetostratigraphy

Three stratigraphic sections were sampled for paleomagnetic analysis in the study area (FP-1, FSCC-1 and M-9). They were selected because of their suitable lithology (red and gray lutites and micritic carbonates), the biochronologic data provided by the paleontologic sites, and their position within the study area (two profiles in the center, and one at the margin of the basin).

A total of 243 m of thickness were sampled, with a total of 259 oriented cores separated by an average distance of 0.9 m. Using previous sedimentation rates calculated for the Baza Basin as a reference (around 5 cm/ka following Garcés et al. (1997) and Oms et al. (1999)), a sampling interval of less than 1 m was established, thus guaranteeing the identification of geomagnetic events lasting less than 100 ka. Samples were collected using an electric drill and cores were oriented in the field using a magnetic compass. Standard paleomagnetic samples were processed in the Paleomagnetic Laboratory at the Institute of Earth Sciences Jaume Almera (CSIC-University of Barcelona). The NRM (Natural Remanent Magnetization) was measured in a three-axis superconducting magnetometer (2G SRM 750). Stepwise thermal demagnetization was applied to all samples in order to determine the different components of the NRM. A Schonstedt TSD1, non-inductive two-chamber furnace was utilized to demagnetize the samples at 50° to 30 °C thermal steps up to 670 °C maximum temperature, corresponding with the complete removal of the remnant magnetization. Magnetic susceptibility (MS) was measured after each temperature step in order to monitor changes in the rock magnetic mineralogy. The observed MS records indicate that no significant mineralogic changes occur upon heating

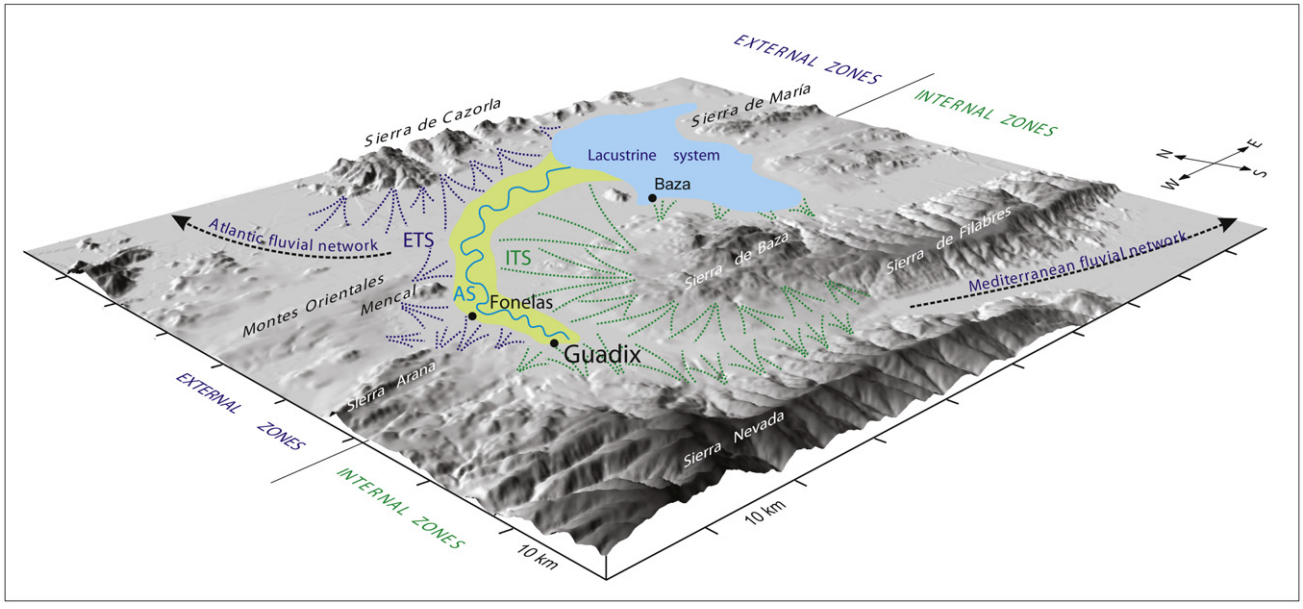

Fig. 3. 3D representation of the paleogeography of the whole Guadix-Baza Depression through the Pliocene and the Pleistocene, showing the spatial distribution of the three main drainage systems: the Axial System (AS), the Internal Transverse System (ITS), and the External Transverse System (ETS).

to 400 °C. Sudden increase of MS at temperatures above 400 °C and a peak at 500 °C points to the formation of significant amount of magnetite during thermal demagnetization. Fortunately, the low residual field (<10 nT) kept in the interior of the demagnetizer did not affect the magnetic remanants through these mineralogic changes.

Stepwise thermal demagnetization results were analyzed by visual inspection of the Zijderveld diagrams (Fig. 4). Most diagrams illustrate the presence in all the samples of a northward-directed component with a maximum unblocking temperature of 300 °C that may represent from 50% to 95% of the NRM. This soft component is subparallel to the present day field and is thus interpreted as a recent overprint acquired during the Brunhes period. At temperatures above 300 °C, samples show a single linear component that gradually decays up to maximum unblocking temperature of 600°–670 °C. This characteristic component is interpreted to have been carried by a mixture of both magnetite and hematite as part of the detrital fraction of the studied sediments. The orientation of the characteristic magnetization yielded a dual-polarity distribution with antipodal normal and reverse polarity means. These results represent a positive reversal which indicates that laboratory treatment was successful in isolating the characteristic component from the recent overprint. Both normal and reverse mean directions yielded inclinations significantly shallower than expected for the geographic latitude of the FP-1, FSCC-1 and M-9 sections. This bias is interpreted as post-depositional flattening of an early acquired detrital remanants, as described by Tauxe (2005). Virtual Geomagnetic Pole (VGP) latitude was calculated for each site in order to establish a Local Magnetic Polarity Stratigraphy (LMPS) of each magnetostratigraphic profile with positive VGP latitudes corresponding to normal polarity magnetization and negative VGP latitudes to reverse polarity magnetization.

4. Stratigraphic scheme

4.1. Lithostratigraphic results

The first step of this study was to map the working area (Fig. 5) and to measure fifteen stratigraphic sections. The second step was a lithologic, sedimentologic, and petrologic study of the sediments of which results have been partially published by Pla-Pueyo et al. (2009a). In order to assign the sediments of the measured profiles to one of the three drainage systems (AS, ITS and ETS) identified in the central sector of the Guadix Basin, two criteria were used. The first was the lithologic composition, while the second was architectural elements characterizing each drainage system in the central sector of the Guadix Basin. The architectural elements identified in the area for each drainage system are described in detail in previous works (Fernández et al., 1991, 1993; Viseras and Fernández, 1992, 1994, 1995; Pla-Pueyo et al., 2007, 2009a,b,c; Pla-Pueyo, 2009). A brief explanation of the lithologic

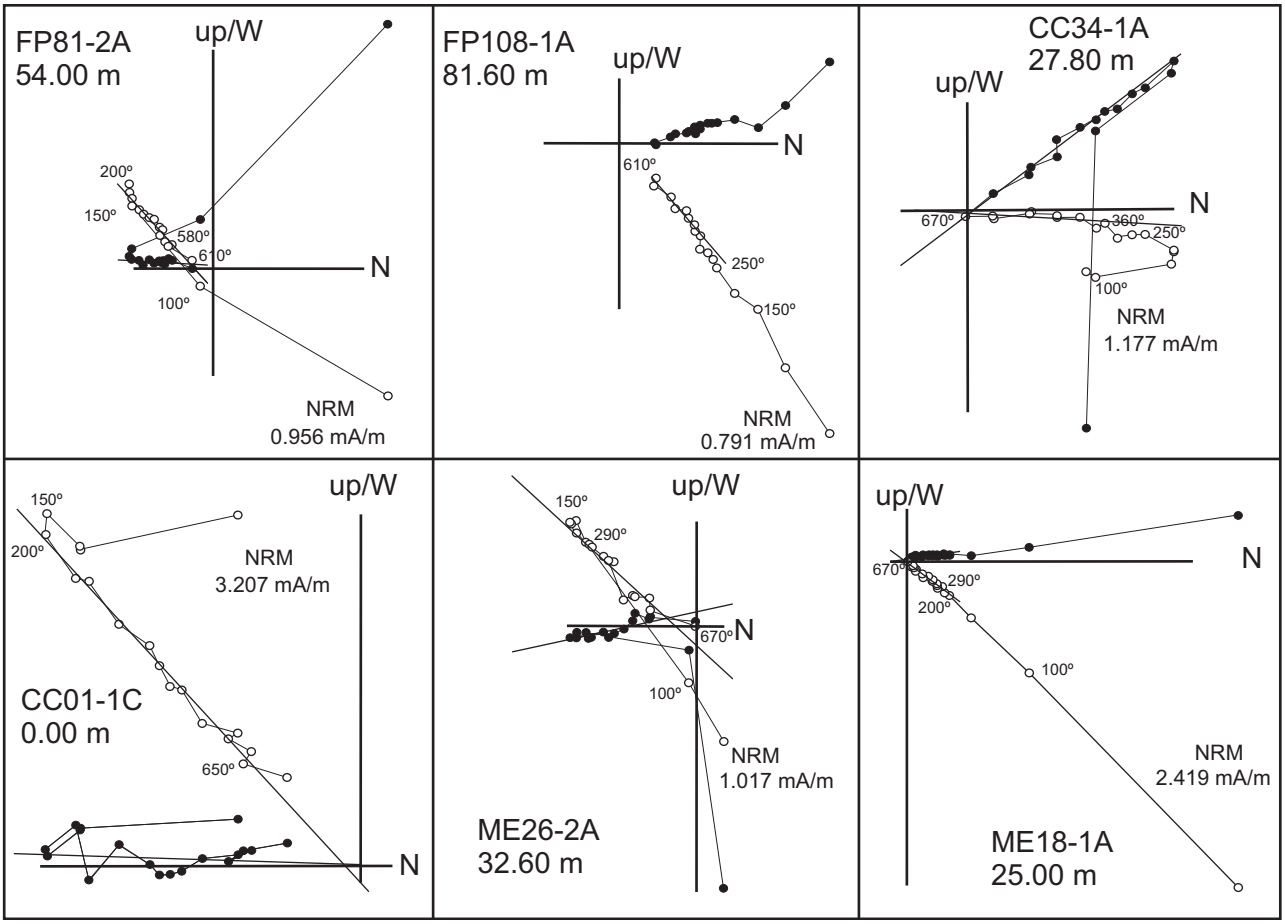

Fig. 4. Examples of Zijderveld diagrams showing the demagnetization vector for some samples from the FP-1, FSCC-1, and M-9 sections. The white and black dots mean vertical or horizontal components respectively.

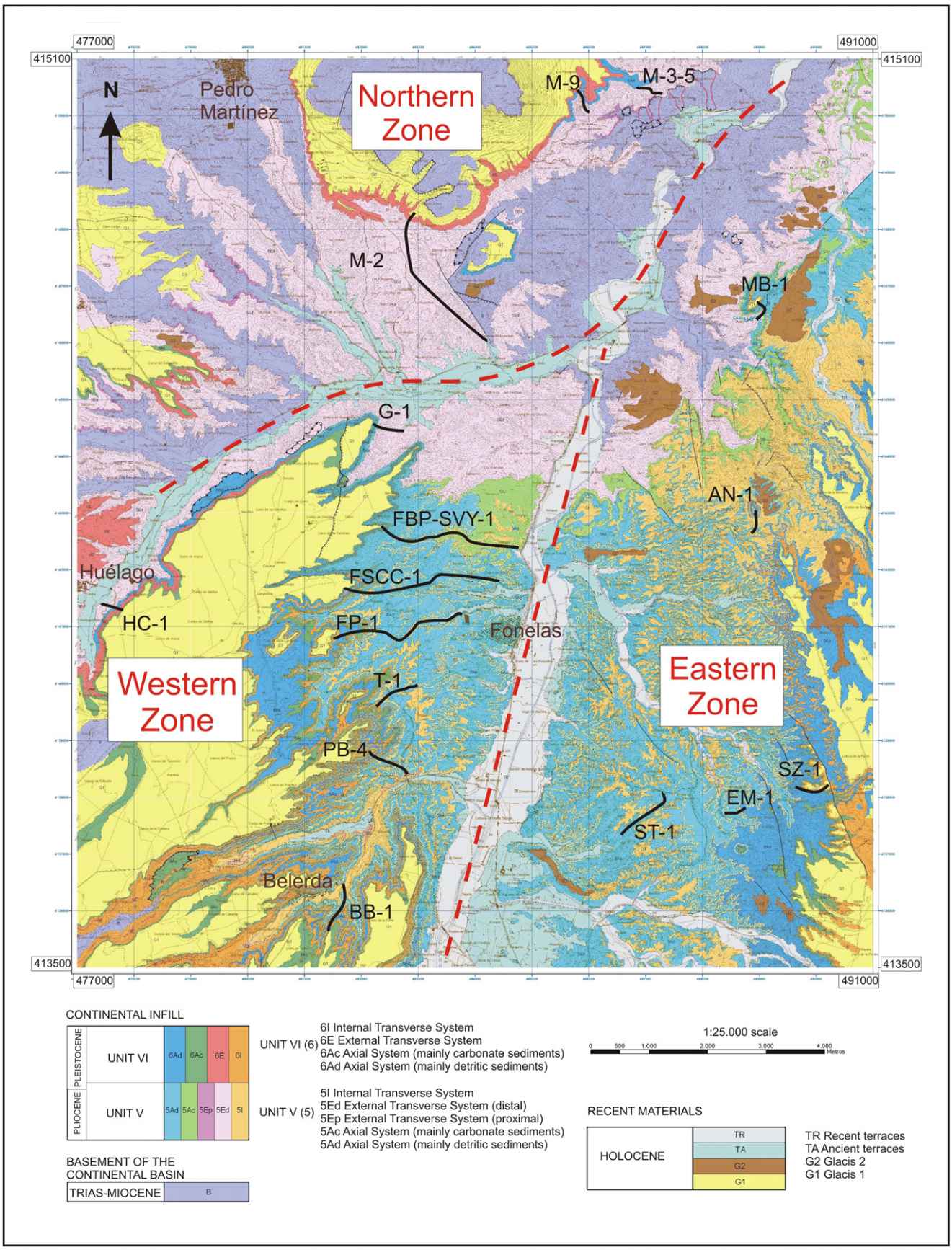

Fig. 5. Geologic map of the central sector of the Guadix Basin (Pla-Pueyo, 2009) showing the study area, divided into three geographic areas (western, northern and eastern zones). The fifteen measured stratigraphic sections are represented by lines, and the different genetic units (V and VI) are represented with different colors. (For interpretation of the references to colour in this figure legend, the reader is referred to the web version of this article.)

composition of the sediments from each drainage system is given below.

4.1.1. Provenance

There are two major source areas for the sediments in the Guadix Basin. They are the External Zones and the Internal Zones of the Betic Cordillera. The External Zones are formed mainly by Mesozoic carbonates, with some intercalated chert beds. The Internal Zones are dominated by metamorphic rocks, showing differences in their composition depending on the complex (Nevado–Filábride Complex, Alpujárride Complex or Maláguide Complex).

Each of the three main drainage systems identified in the working area exhibit a characteristic lithology. Therefore, it is relatively easy to identify the source area, and consequently, the original drainage system, when observing the lithologic composition of the sediment in the central sector. This is quite important in terms of correlating beds deposited in association with the same drainage system.

The resultant depositional lithology present in the three drainage systems (AS, ITS, and ETS) has been previously described (Fernández et al., 1991, 1993; Viseras and Fernández, 1992, 1994, 1995; Pla-Pueyo et al., 2009a). The sediments of the AS are dominated by the characteristic metamorphic lithology typical of the Internal Zones (mainly quartzites and mica schists from the Nevado–Filábride Complex). The Internal Transverse System (ITS) shows the same metamorphic-dominated lithology, but it also contains a considerable proportion of dolomitic marbles coming from the Alpujárride Complex, belonging to the Internal Zones as well. In contrast, the External Transverse System non-metamorphic sediments are mainly carbonates, with some chert.

4.1.2. Stratigraphic sections

A total of fifteen stratigraphic sections were measured within the study area (see Fig. 5). Some of these sections were measured across the most important paleontologic sites (profiles FPB-4, FP-1, FSCC-1, FBP-SVY-1, M-3-5, M-8, M-9, ST-1 and SZ-1) while the rest have intermediate positions in order to facilitate the lithostratigraphic correlation (profiles BB-1, T-1, G-1, M-2, MB-1 and AN-1).

Three geographic zones may be differentiated within the study area, divided by recent valleys (Fig. 5): the western, northern and eastern zones. The western zone hosts the stratigraphic sections BB-1, FPB-4, T-1, FP-1, FSCC-1, FBP-SVY-1 and G-1. The most common feature in these sections is the predominance of sediments from the AS alternating with ITS sediments. Only the sections that are geographically closest to the External Zones (BB-1 and G-1) present a significant amount of sediments of the ETS. The northern zone is close to the margin of the basin limited by the External Zones. Therefore, the three sections measured in this zone (M-2, M-9 and M-3-5) show a high proportion of ETS sediments. No sediments of the ITS were found in these sections. The sections of the eastern zone (AN-1, SZ-1 and ST-1) exhibit, as the western zone, alternating sediments from the AS and the ITS, and only in the northernmost section (MB-1) is the proportion of ETS sediments important. Only the three stratigraphic sections that underwent paleomagnetic analysis will be described in detail below.

4.1.2.1. FP-1. The *Fonelas P-1* section is significant since it hosts the large-mammal site Fonelas P-1 (Garrido, 2006; Viseras et al., 2006; Arribas and Garrido, 2007; Arribas, 2008; Garrido and Arribas, 2008; Arribas et al., 2009). It is located in the center of the basin in a highly subsiding zone. Its 118 m of sediments correspond mainly to the floodplain of the Axial System (AS), dominated by fluvial, grayish, medial-distal siliciclastic facies and palustrine carbonates (Fig. 6A). Intercalated cyclically are ITS red alluvial sediments.

4.1.2.2. FSCC-1. The *Fonelas Solana Cortijo del Conejo-1* section is named after one of the paleontologic sites that it hosts. It is approximately 1 km farther north from FP-1 profile. The thickness of 146 m exhibits a very similar facies distribution to FP-1 (Fig. 6.B.) and can be easily correlated to it by bed–bed correlation. Three biochronologically important paleontologic sites appear in this section: FSCC-1, FSCC-2 and FSCC-3.

4.1.2.3. M-9. The *Mencal-9* section is located close to the northern margin of the Guadix basin. Its 105 m can be divided into three intervals (Fig. 6C). The lowest and the uppermost correspond to pinkish carbonate sediments of the ETS, while the intermediate interval is formed by gray to white siliciclastic and carbonate floodplain sediments of the AS. Within these floodplain sediments, the M-8 and M-9 paleontologic sites occur.

4.1.3. Lithostratigraphic correlation

The correlation based on stratigraphic and sedimentologic criteria led to a lithostratigraphic correlation among the fifteen stratigraphic sections. Three inferences that could be extracted from this correlation include:

(1) The predominance of fine-grained sediments in the study area and the type of architectural elements characterizing each drainage system, shows that the central sector of the Guadix Basin occupies a relatively distal position within the Axial System. Moreover, sediments interpreted as the medial-distal facies of the ITS and ETS alluvial fans are present (Viseras and Fernández, 1992; Fernández et al., 1996b; Pla-Pueyo et al., 2009a).
(2) The most important large-mammal sites appear associated with the AS fluvial system. Within the established lithostratigraphic correlation scheme, a relative age can be inferred. Therefore, the order of the sites from the oldest to the youngest would be: FSCC-3, FSCC-2, ST-1, FPB-4, FP-1, FSCC-1, FBP-SVY-1, M-8, M-9, M-5, M-4 and M-3. In this first step, the stratigraphic interpretation and the relative age deduced for the sites agreed with the previous biochronologic interpretation established for some of the paleontologic sites, such as FPB-4, FP-1, FSCC-1 and FSCC-2 (Viseras et al., 2006; Arribas et al., 2009).
(3) There is a lithologic and sedimentologic change between the lower and medial part and the uppermost part of the sections. A surface separating these two different sedimentary stages was identified and it has been interpreted to be the boundary between genetic units V and VI, which was not clearly defined in previous research on the central part of the Guadix Basin.

4.2. Previous biostratigraphic framework

The biochronologic information used as a reference for the paleomagnetic analysis has been entirely provided by the paleontologic team of the Fonelas Project (Viseras et al., 2006; Arribas and Garrido, 2007; Garrido and Arribas, 2008; Arribas et al., 2009, among others). The fossil remains appear mainly in the Axial System fluvial sediments, within a 6 m-thick sediment interval that comprises a total volume of 240 000 000 m^3 of continental sediments within the Pleistocene (using the Pliocene-Pleistocene boundary as defined in the International Stratigraphic Chart, International Stratigraphic Chart IUGS, 2009). These fossiliferous units in this strip have a minimum area of 40 km^2.

The fossil remains appear mainly in the Axial System fluvial sediments, within a 6 m-thick sediment interval, outcropping in an area of about 40 km^2 that would comprise a total volume of about 240 hm^3 of continental sediments within the Pleistocene.

From a biostratigraphic point of view, the most interesting large-mammal sites in the central sector of the Guadix Basin are

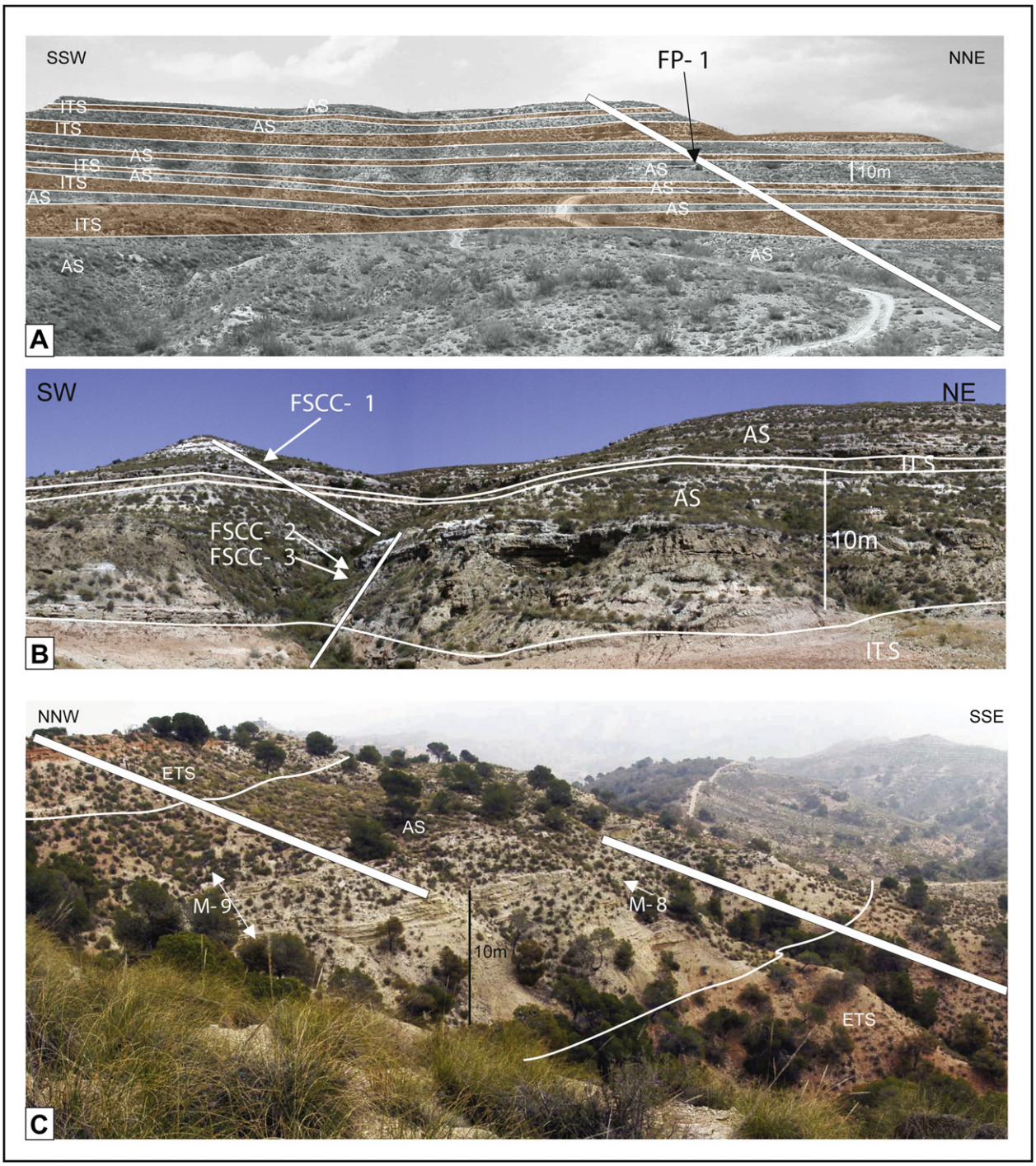

Fig. 6. Stratigraphic interpretations of FP-1 (6.A.), FSCC-1 (6.B.), and M-9 (6.C.) sections showing the different sediment groups corresponding to each drainage system (ITS: Internal Transverse System; AS: Axial System; ETS: External Transverse System). A white bar indicates part of the approximate path followed to measure each profile. The position of some of the macromammal sites is also indicated.

FSCC-3, FSSC-2, FPB-4, FP-1, FSCC-1, FBP-SVY-1 and M-9. The faunal association of each site (Table 1) were delineated by the paleontologic team into mammal zones (following the nomenclature of Guérin, 1982, 1990) ranging from MNQ17 to MNQ20 (Arribas et al., 2009). This information was used when correlating the magnetozones of the three magnetostratigraphic profiles to the GTPS (Lourens et al., 2004).

4.3. Magnetostratigraphic results

Once a detailed lithostratigraphic correlation scheme was developed, FP-1, FSSC-1 and M-9 sections were selected for paleomagnetic sampling. The aim of this sampling was to confirm the quality of the previous correlation and to obtain a time frame in the study zone, reflecting the evolution of the sedimentary infilling.

Table 1
Faunal association of the main paleontologic sites within the three sections sampled for paleomagnetic analysis. All the information in this table is taken from Arribas et al.(2009).

CLASS/ORDER		PALEONTOLOGIC SITES						
		FPB-4	FP-1 (trench B)	FSCC-3	FSCC-2	FSCC-1	FBP-SVY-1	M-9
Amphibia						*Anura* gen. indet.		
Reptilia			*Lacertidae* gen. indet *Anguidae* gen. indet. *Rhinechis scalaris* *Viperidae* gen. indet. *Eurotestudo* sp.					*Quelonia* gen. indet.
Aves			*Aves* gen. indet.			*Aves* gen. indet.		
Mammalia	Rodentia		*Mimomys* sp. *Castillomys* sp. gr. *C. crusafonti* *Apodemus cf. atavus* *Stephanomys* sp. *Eliomys* sp.					
	Insectivora Lagomorpha		*Erinaceinae* gen. indet. *Oryctolagus* sp. *Prolagus cf. calpensis*			*Oryctolagus* sp.		
	Carnivora	*Canidae* gen. indet. *Chasmaporthetes lunensis*	*Meles iberica* *Vulpes alopecoides* *Canis accitanus* *Canis etruscus* *Canis cf. falconeri* *Pachycrocuta brevirostris Hyaena brunnea* *Lynx issiodorensis valdarnensis* *Acinonyx pardinensis* *Megantereon cultridens roderici* *Homoterium latidens*			*Canis etruscus* *Lynx* sp. *Megantereon* sp. *Hyaena brunnea* *Pachycrocuta brevirostris*		
	Artiodactyla	*Eucladoceros* sp. *Gazellospira* sp. *Leptobos* sp.	*Potamochoerus magnus* *Croizetoceros ramosus fonelensis* *Metacervoceros rhenanus philisi* *Eucladoceros* sp. *Mitilanotherium* sp *Gazellospira torticornis hispanica* *Capra baetica* *Praeovibos* sp.		*Gazella borbonica*	*Metacervoceros rhenanus philisi* *Gazellospira* sp. *Leptobos etruscus* *Praeovibos* sp.	*Metacervoceros rhenanus perolensis*	*Bovini* gen. indet.
	Perissodactyla	*Equus* sp.	*Equus cf. major* *Stephanorhinus etruscus*			*Equus cf. major* *Equus* sp.		*Equus* sp.
	Proboscidea		*Mammuthus meridionalis*	*Anancus* sp.		*Mammuthus meridionalis*		*Mammuthus cf. meridionalis*

The entire FP-1 section was sampled, and 135 samples were taken from its 118 m. The average space between samples is 90 cm (Fig. 7). In the case of FSCC-1, only the 45 m that host the three large-mammal sites (FSCC-1, FSCC-2 and FSCC-3) were sampled. As a result, 54 samples were obtained, with an average space between them of 80 cm (Fig. 8).

Finally, M-9 section was sampled in its upper 80 m, and 70 samples were obtained. The average space between them (110 cm) is higher than in the other two profiles because of the nature of the sediments (Fig. 9). Two of the three lithologic intervals forming this section are composed of alluvial fan sediments of the ETS (see also Fig. 6C). Taking into account the sedimentation style of this system (conglomeratic bodies alternating with lutitic/marly beds), this means that the grain size of the sediment is more heterogeneous in comparison to the floodplain sediments of the AS. Therefore, it was more difficult to find suitable sediment for sampling.

When processed in the laboratory, the NRM (Natural Remanent Magnetization) of the samples was intense. Once the viscose component was eliminated, the average magnetization was 5.3 mA/m for the samples collected in FP-1 and 2.2 mA/m in M-9. Minimum and maximum values of magnetization corresponded to limestones and red/pink sands, respectively, while the relatively high remanence average (20 mA/m) was representative of gray sandy silt, the most abundant sampled lithology within the Axial System facies. The analysis has revealed the existence of a stable or characteristic magnetization, with the presence of normal and reverse polarities and a range of unblocking temperatures between 600° and 670 °C (see Fig. 4). The high magnetization is attributed to the siliciclastic input from the Internal Zones, rich in iron oxides (magnetite and hematite).

5. Discussion

5.1. Correlation of the sampled profiles

The three magnetostratigraphic profiles obtained from FP-1, FSCC-1 and M-9 sections can be correlated (Fig. 10). The

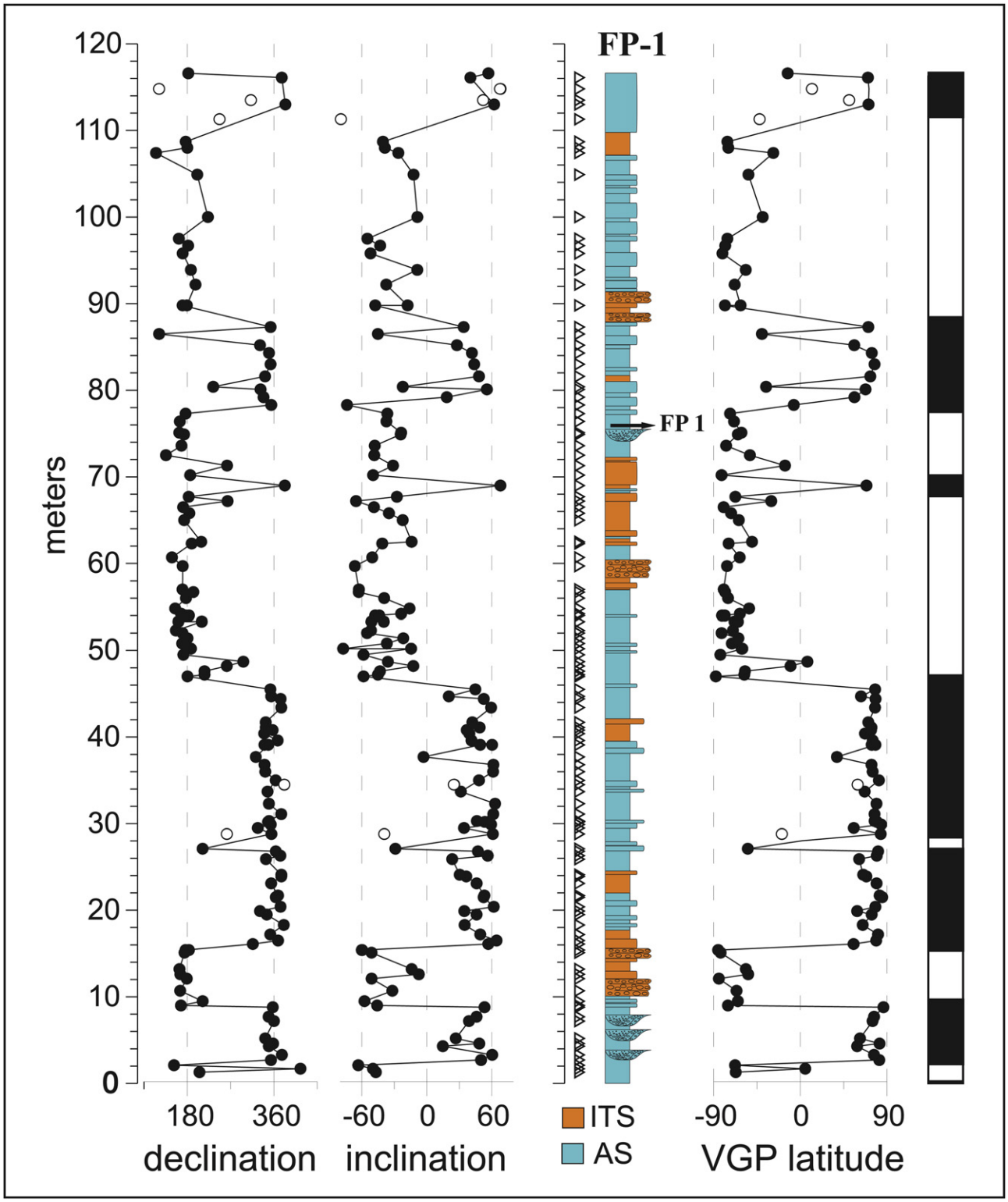

Fig. 7. Magnetostratigraphy of FP-1 section. In the stratigraphic section, the position of the FP-1 site (trench B) is indicated. Sediments belonging to the Axial System are represented in blue, while than those related to the Internal Transverse System are represented in orange. Starting from the characteristic declination and inclination of each sample, the virtual magnetic pole (VGP) latitude was calculated. Negative values of the VGP latitude represent reverse polarity (white), while positive values represent normal polarity (black). Black dots represent reliable directions used for the magnetostratigraphy while white dots mark the position of discarded unsuitable samples. See also Fig. 6A. (For interpretation of the references to colour in this figure legend, the reader is referred to the web version of this article.)

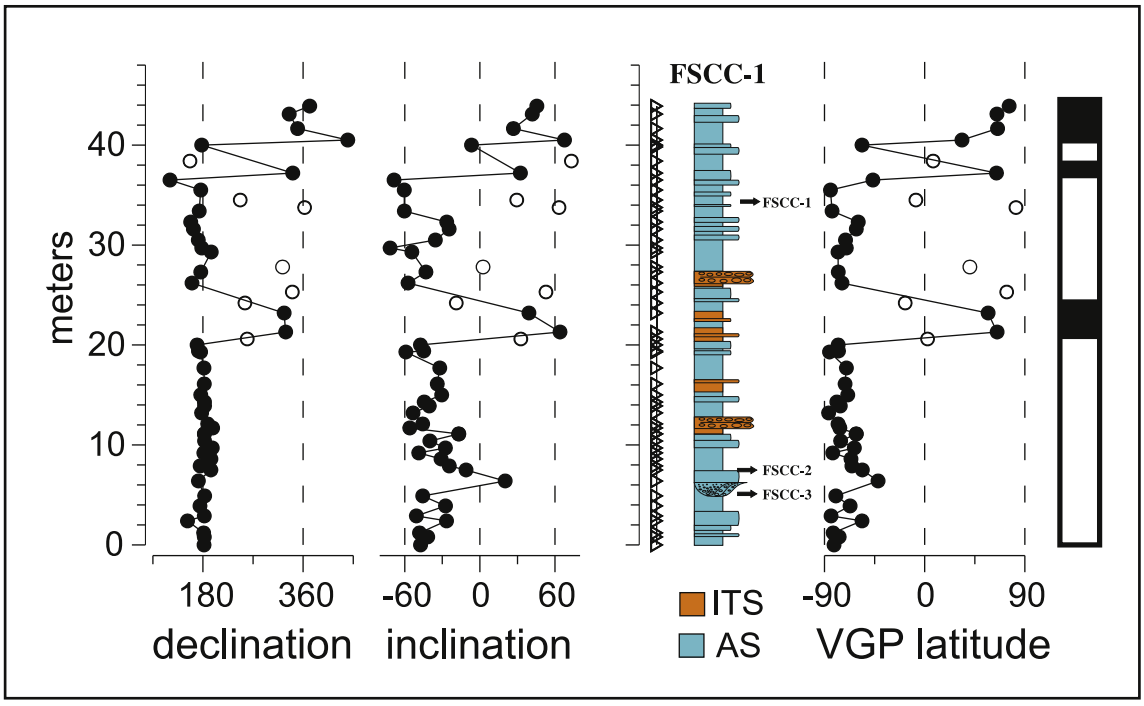

Fig. 8. Magnetostratigraphy of the FSCC-1 section The position of FSCC-1, FSCC-2 and FSCC-3 sites is indicated. Sediments belonging to the Axial System are represented in blue while those related to the Internal Transverse System are represented in orange. Black dots represent reliable directions used for the magnetostratigraphy while white dots mark the position of discarded unsuitable samples. See also Fig. 6.B. (For interpretation of the references to colour in this figure legend, the reader is referred to the web version of this article.)

characteristic pattern given by the reverse magnetozones, especially in the case of FP-1 and M-9, together with the previous biochronologic information obtained from the main sites (see Table 1), allows a feasible correlation with the GPS2004 (Gibbard and Van Kolfschoten, 2004; Lourens et al., 2004).

When a chron has been attributed to a single site (such as the ones at stratigraphic heights of 27 m and 69 m) or has been considered part of a larger chron with a different general polarity (such as sites at stratigraphic heights 80 and 86 m) it is due not only to their paleomagnetic correlation, but also to the biochronologic information and the lithostratigraphic correlation bed to bed carried out between the three sampled profiles and the rest of the stratigraphic measured sections.

Although the paleomagnetic data obtained for FP-1 section have been recently published (Arribas et al., 2009), a description of all three magnetostratigraphic profiles is provided below to give a general overview of the magnetostratigraphy. The three thick normal magnetozones in the lower part of FP-1 and M-9 are correlated to the Gauss interval (C2An), followed by a mainly reverse interval, appearing in all three profiles, corresponding to the Matuyama interval (Fig. 10). The normal magnetozone located stratigraphically over paleontologic sites FP-1, FSCC-1 and including M-8 site represents the normal polarity chron Olduvai (C2n). Reunion Chron (C2r.1n) is identified as a normal magnetozone that can be correlated between FP-1 and FSSC-1 sections. The reverse magnetozone over Olduvai Chron (C2n) encompasses the C1r.3r, C1r.2n (Cobb Mountains) and C1.2r chrones because the short middle Cobb Mountain has not been identified in any of the sampled sections. The magnetic polarity sequence obtained for M-9 section is quite similar to the one for FP-1, except for the absence of the Reunion Chron. This is probably due to the longer spacing between samples or differences related with sedimentation rates (M-9 section is located in a tectonic horst area, while FP-1 and FSCC-1 are located in a subsiding zone) (Pla-Pueyo et al., 2009a), influencing the record resolution. Another difference between the FP-1 and M-9 magnetostratigraphic profiles is the presence of a normal magnetozone in M-9 that is not recorded in FP-1. This magnetozone has been interpreted as the Jaramillo Chron (C1r.1n).

The topmost magnetozone identified in both FP-1 and M-9 profiles is interpreted as the Brunhes Chron (C1n). This interpretation is supported by the presence of the archeologic site Solana del Zamborino (e.g., Botella et al., 1975; Scott and Gibert, 2009) within the sediments deposited at the end stage of the basin fill (unit VI) and its lithostratigraphic correlation with the rest of the sites in the study area.

There are also other reasons to support this assumption. If the magnetozones are observed in terms of thickness, then the Jaramillo Chron in M-9 would be 50 cm thick and the Brunhes would be 10 m thick. In FP-1 section, the topmost normal magnetozone is 6 m thick. If Jaramillo and Brunhes chrons are recorded in the M-9 section, then it is more reasonable for the topmost magnetozone, Brunhes, to be the same in both M-9 and FP-1.

Erosion would have reduced the thickness of Brunhes in the FP-1 section. The absence of Jaramillo in the upper part of FP-1, where this chron would be expected to appear, may be due to the presence of palustrine deposits (which are discontinuous in time).

The data that can be inferred directly from the three sampled profiles are the ages of the paleontologic sites hosted in FP-1, FSCC-1 and M-9 and the time range for sedimentation corresponding to each magnetozone in each section. After the correlation with the GPTS scale (Fig. 10), the large-mammal site Fonelas P-1, hosted by the FP-1 section, is 2.0 Ma old. The ages for the three sites in FSCC-1 section are 2.5–2.4 Ma for FSCC-2 and FSCC-3 and 2.0 Ma for FSCC-1, slightly younger than FP-1 site. In the M-9 section, the M-8 site has an age range of 1.9–1.8 Ma, while the M-9 site is between 1.6 and 1.4 Ma.

Starting from these data, it was possible to calculate sedimentation rates and to compare their spatial distribution and their change during the deposition of sediments forming FP-1 and M-9, assuming that FSCC-1 represents in general the same values as FP-1

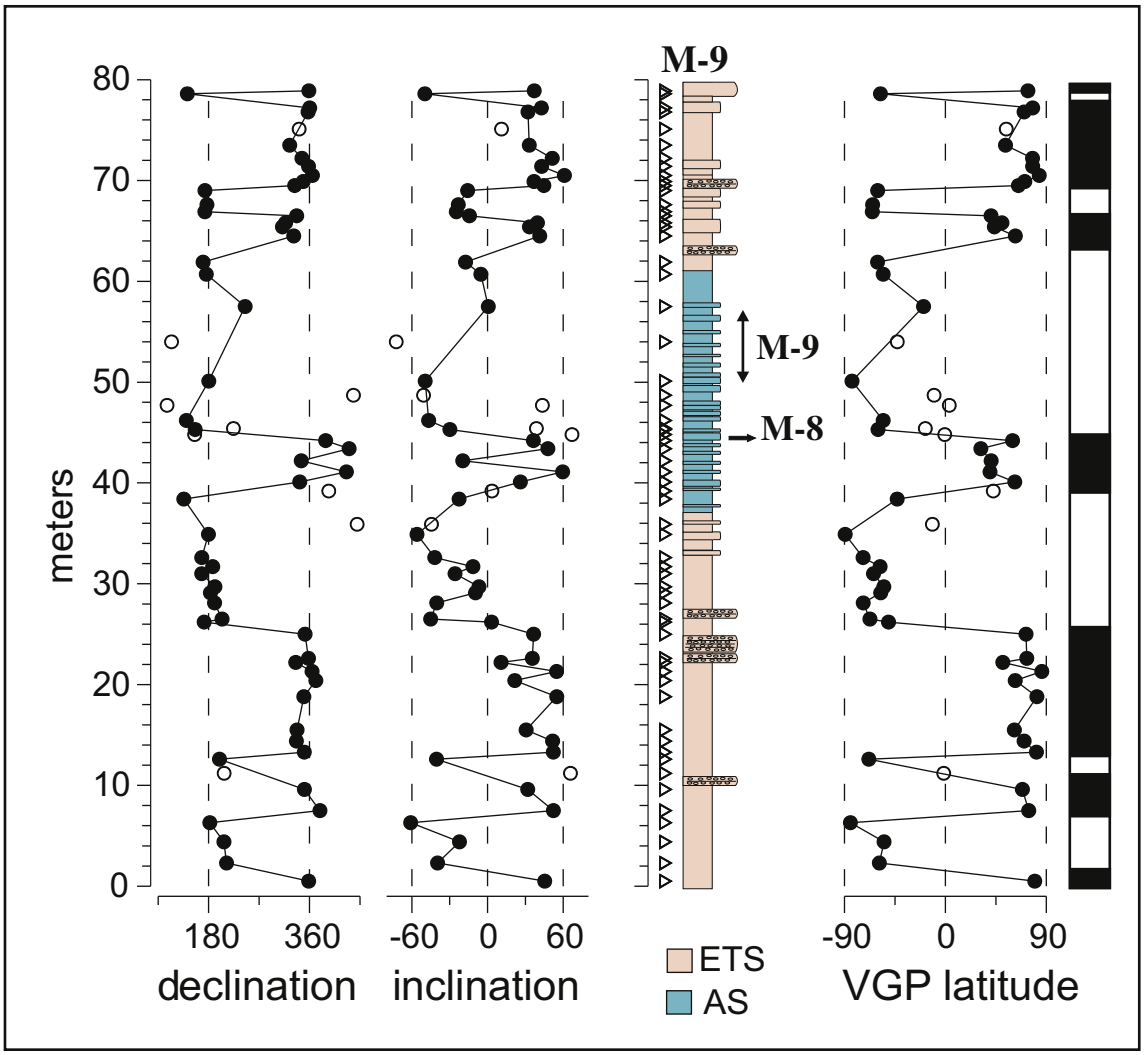

Fig. 9. Magnetostratigraphy of M-9 section. The position of the M-8 and M-9 sites is indicated. Sediments belonging to the Axial System are represented in blue while those related to the External Transverse System are represented in pink. Black dots represent reliable directions used for the magnetostratigraphy while white dots mark the position of discarded unsuitable samples. See also Fig. 6C. (For interpretation of the references to colour in this figure legend, the reader is referred to the web version of this article.)

(Pla-Pueyo et al., 2009a). The calculations of the sedimentation rates in the sampled time interval show a sudden decrease in the sedimentation rates at the age of 1.778 Ma, which corresponds to the boundary between normal Chron C2n (Olduvai) and C1r. The average sedimentation rate for sediments older than 1.778 Ma is 5.2 cm/ka in FP-1 section (center of the basin) and 3 cm/ka in M-9 section (margin of the basin). In contrast, for the sediments younger than 1.778 Ma, the average sedimentation rate is quite similar in the center (2.4 cm/ka) and in the margin (2.3 cm/ka) of the basin (Pla-Pueyo et al., 2009a). This decrease coincides with a lithologic change in the AS facies from a siliciclastic-dominated sedimentation to a deposition in which palustrine-lacustrine carbonates are predominant. In general, there is also a change in the style of the architectural elements for the three drainage systems, changing from elements typical of a high accommodation space situation to those indicating low accommodation space available (Pla-Pueyo, 2009).

Therefore, combining the lithostratigraphic and the paleomagnetic data, a new position of the boundary between units V and VI is proposed for the center of the Guadix Basin (see Fig. 5), with an age of 1.778 Ma (Pla-Pueyo et al., 2009a). The position of the boundary had not been previously precisely identified in the center of the basin, because of the continuity of the sedimentation in the Axial System sediments distally. This boundary represents a tectonic change, reflected in a decrease of the sedimentation rates in the Guadix Basin, and producing an unconformity at the margins of the basin (Viseras, 1991; Fernández et al., 1996a, b; Soria et al., 1998; Viseras et al., 2005), together with the displacement northwards of the paleogeographic axis of the basin and a drastic shift in the sedimentation styles from unit V to unit VI.

5.2. Extrapolation of the magnetostratigraphic data to the lithostratigraphic framework

The integration of the three magnetostratigraphic profiles with the lithostratigraphic correlation, with the previous biostratigraphic information, led to a more precise stratigraphic framework for the paleontologic sites located in the area (Fig. 11A,B). As a result, a number of isochronous surfaces have been traced, extrapolating the data from the three sampled sections to the rest of the fifteen sections. The extrapolation of the boundary between units V and VI was a very helpful tool to define the rest of the isochronous surfaces.

For the eastern zone of the central sector, with rare paleontologic sites containing biochronologic information, the main criteria used to extrapolate the isochronous surfaces has been the position

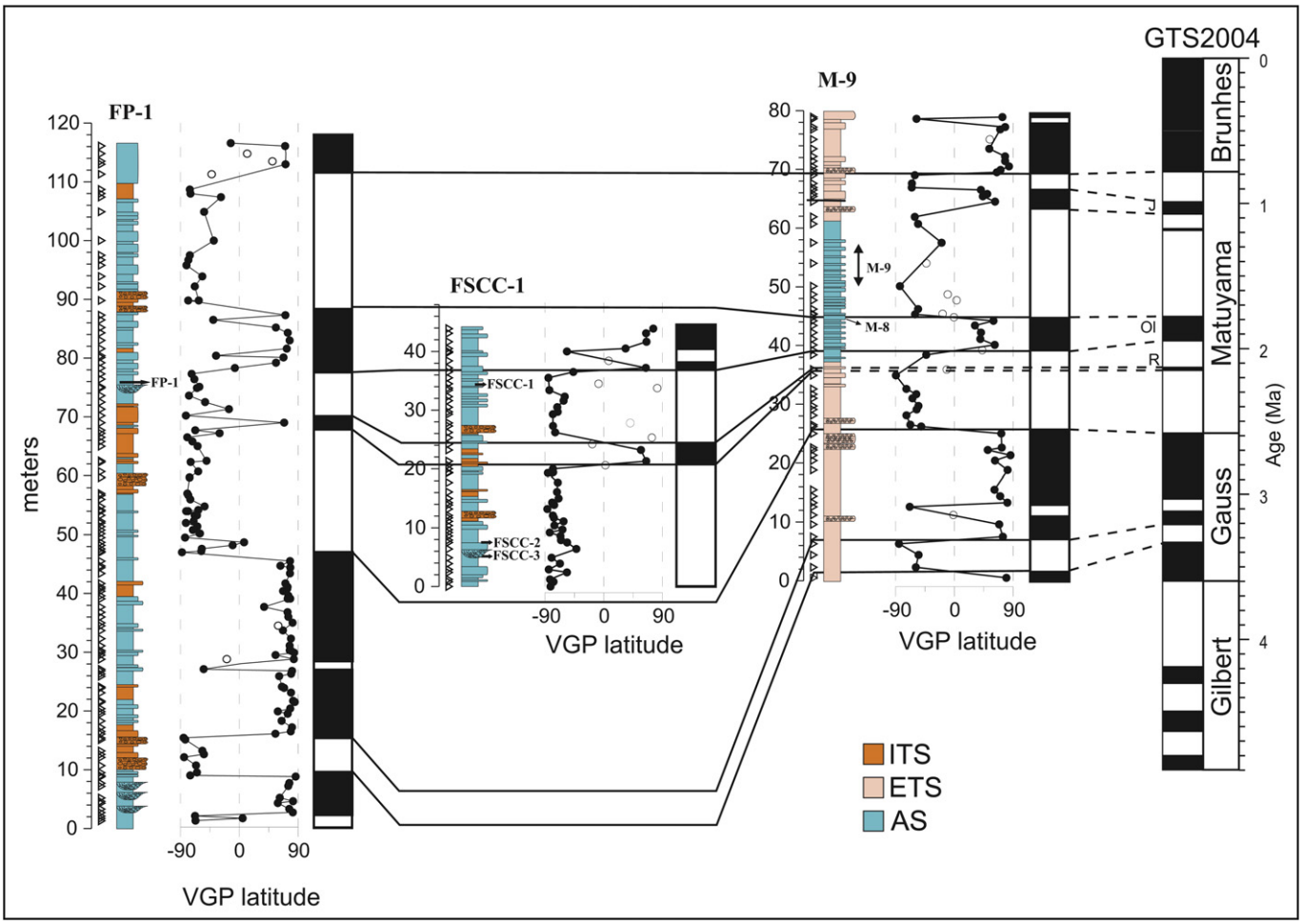

Fig. 10. Magnetostratigraphic correlation among the FP-1, FSCC-1 and M-9 sections, and the GTS2004 (Lourens et al., 2004). Black dots represent reliable directions used for the magnetostratigraphy while white dots mark the position of discarded unsuitable samples.

of each ITS intercalation within the facies of the AS. The sixteen intercalations appearing in the western zone have been also identified in the eastern zone. They correspond to the prograding facies of the ITS. Therefore, the isochronous surfaces have been extrapolated to the eastern zone of the central sector through their relative position with respect to the intercalations in the western zone.

Using the litho-, bio- and magnetostratigraphic scheme presented (Fig. 11A,B), the extrapolated ages of the paleontologic sites from the oldest to the youngest is approximately as follows: between the estimated age for FSCC-2 and FSCC-3 sites (2.5–2.5 Ma, stratigraphically higher than them) and 2.148 Ma (the bottom of the Reunion Chron) for ST-1 site; 2.128–2.0 Ma (reverse polarity between Chron C2r.1r (Reunion) and FP-1 site) for FPB-4; and 1.778–1.072 Ma (reverse polarity between Olduvai and Jaramillo Chrons) for the zone where M-3, M-4, and M-5 appear. The age of paleontologic site ST-1, located in the eastern zone of the central sector, has been interpreted through its relative position to intercalations 6 and 9. For the Solana del Zamborino site (Botella et al., 1975; Scott and Gibert, 2009, among others), the correlation agrees with the archeologic data and is interpreted to be within the Bruhnes epoch, as it is between intercalations 14 and 15, closer to intercalation 15. The position of SZ-1 within the Bruhnes epoch is also proposed by other authors (Scott and Gibert, 2009). However, this extrapolation does not allow an estimation of a numerical age for the site.

6. Final remarks

The stratigraphic, sedimentologic and petrologic studies of units V and VI and geologic mapping of the central sector of the Guadix Basin have led to the following conclusions.

(1) Several isochronous surfaces have been established for the central sector of the Guadix Basin, resulting from the integration of the magnetostratigraphic results in a previous lithostratigraphic scheme.
(2) A numerical age has been obtained for the most important large-mammal sites of the Fonelas Project located within the study area. Arranged chronologically from the oldest to the youngest, the sites have the following ages:
   - 2.5–2.4 Ma for FSCC-2 and FSCC-3.
   - Between 2.5 and 2.4 Ma (stratigraphically higher than FSCC-2 and FSCC-3) and 2.148 Ma (under the beginning of the Reunion Chron) for ST-1 site.
   - 2.128–2.0 Ma (reverse polarity between Chron Reunion and FP-1 site) for FPB-4.

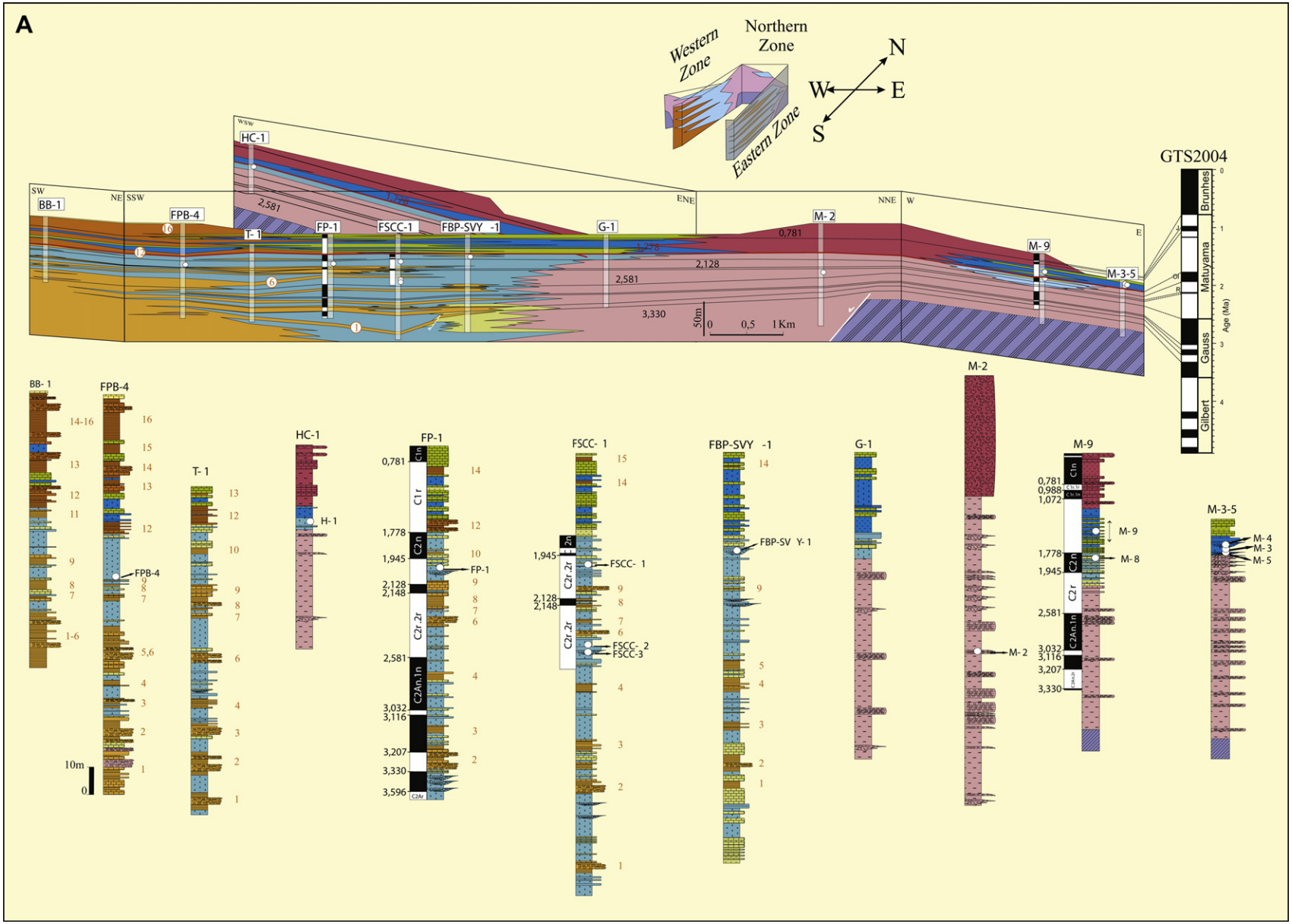

Fig. 11A. Correlation scheme using litho-, bio- and magnetostratigraphic data from the western and northern zones of the central sector of the Guadix Basin. The lines crossing the diagram horizontally are isochronous, extrapolated from the paleomagnetic data. The thick line at the top of the normal polarity Chron marked Olduvai is the boundary between Units V and VI.

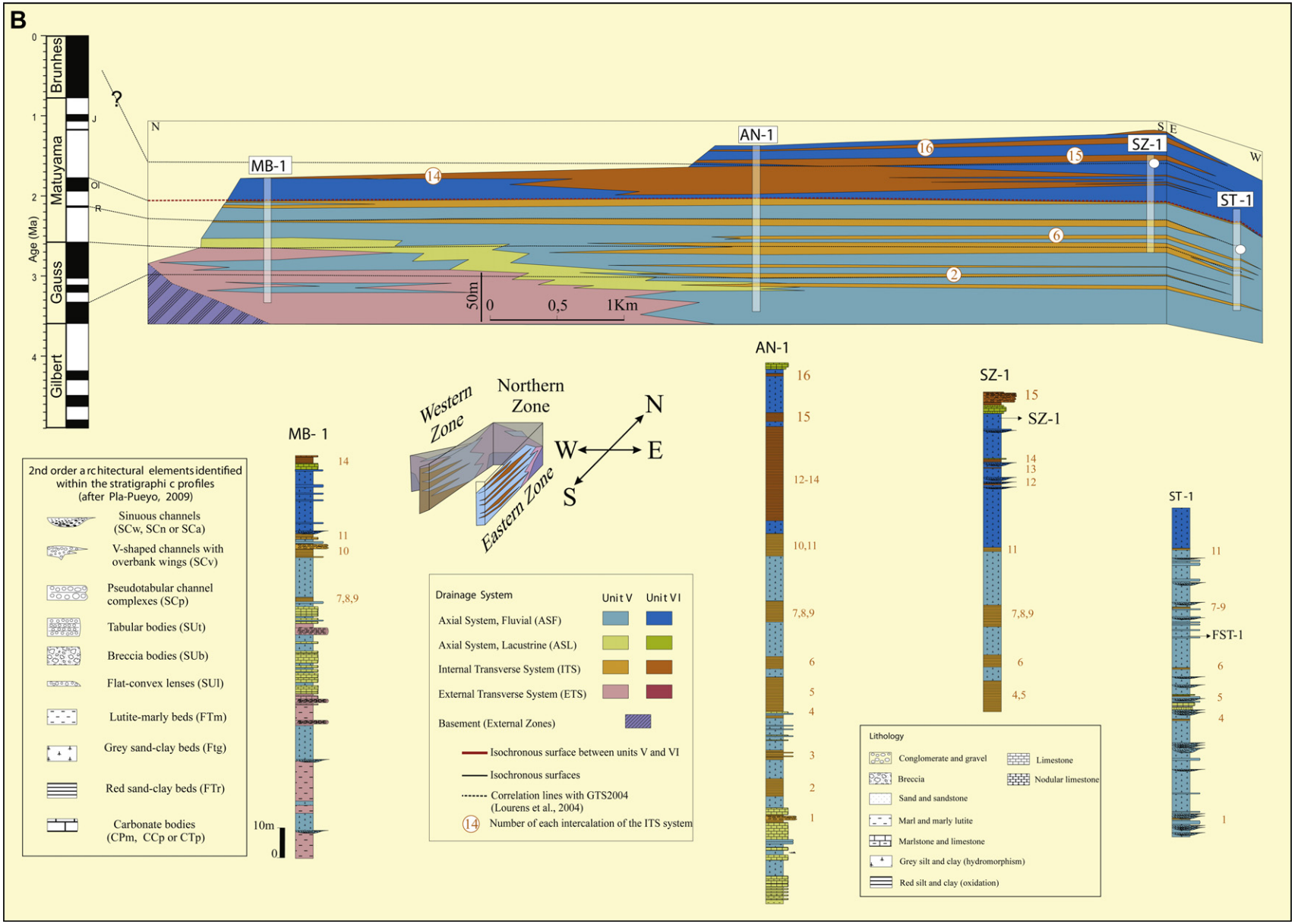

Fig. 11B. Correlation scheme using litho-, bio- and magnetostratigraphic data from the eastern zone of the central sector of the Guadix Basin. The black lines crossing the diagram horizontally are isochronous, extrapolated from the paleomagnetic data. The thick red line at the top of the normal polarity chron marked Olduvai is the boundary between Units V and VI (For interpretation of the references to colour in this figure legend, the reader is referred to the web version of this article.).

- 2.0 Ma for FP-1 and FSCC-1, the first one slightly older than the second one.
- 1.9 Ma (normal polarity, beginning of Olduvai Chron) for FBP-SVY-1.
- 1.9–1.8 Ma for M-8.
- 1.778–1.072 Ma (reverse polarity between Olduvai and Jaramillo Chrons) for the zone where M-3, M-4, and M-5 appear.
- 1.6–1.4 Ma for M-9.

(3) An age of 1.778 Ma has been inferred for the isochronous surface representing the boundary between genetic units V and VI of the infill of the Guadix Basin.

Acknowledgments

We want to thank Jose Antonio García Solano for his help during the paleomagnetic sampling. Paleomagnetic analyses (record number 563/06) were carried out at the Paleomagnetic Laboratory of the University of Barcelona and the Institute of Earth Sciences (CSIC) of Barcelona, and they were funded by the Fonelas Project (Spanish Geological Survey, I.G.M.E.) by means of a service contract (report number 2006/11). We are also grateful to Dr. Elizabeth Gierlowski-Kordesch for her kindness in reviewing the English. The first author is currently enjoying a contract from the University of Granada. The present research is funded by Research Group RNM369, and by research projects CGL2009-05768-E/BTE, CGL2009-07830/BTE and IGME 2001-016.

References

Agustí, J., Cabrera, L., Garcés, M., Krijgsman, W., Oms, O., Parés, J.M., 2001a. A calibrated mammal scale for the Neogene of western Europe. State of the art. Earth Science Reviews 52 (4), 247–260.

Agustí, J., Oms, O., Garcés, M., Parés, J.M., 1997. Calibration of the late Pliocene–Early Pleistocene transition in the continental beds of the Guadix-Baza basin (South-Eastern Spain). Quaternary International 40, 93–100.

Agustí, J., Oms, O., Parés, J.M., 1999. Calibration of the early-middle Pleistocene transition in the continental beds of the Guadix-Baza basin (SE Spain). Quaternary Science Reviews 18, 1409–1417.

Agustí, J., Oms, O., Remacha, E., 2001b. Long Plio-Pleistocene terrestrial record of climate change and mammal turnover in southern Spain. Quaternary Research 56, 411–418.

Andrieux, J., Fontboté, J.M., Mattauer, M., 1971. Sur un modèle explicatif de l'Arc de Gibraltar. Earth and Planetary Science Letters 12 (2), 191–198.

Vertebrados del Plioceno superior terminal en el suroeste de Europa: Fonelas P-1 y el Proyecto Fonelas. Instituto Geológico y Minero de España. In: Arribas, A. (Ed.), serie Cuadernos del Museo Geominero, 10, p. 607.

Arribas, A., Garrido, G., 2007. *Meles iberica* n. sp., a new Eurasian badger (Mammalia, Carnivora, Mustelidae) from Fonelas P-1 (Plio-Pleistocene boundary, Guadix basin, Spain). Comptes Rendus Palevol 6, 545–555.

Arribas, A., Garrido, G., Viseras, C., Soria, J.M., Pla-Pueyo, S., Solano, J.G., Garcés, M., Beamud, E., Carrión, J., 2009. A mammalian lost world in Southwest Europe during the late Pliocene. Plos One 4 (9), 1–10. e7127.

Barnosky, A.D., Bibi, F., Hopkins, S.S.B., Nichols, L., 2007. Biostratigraphy and magnetostratigraphy of mid-Miocene railroad Canyon Sequence, Montana and Idaho, and age of the Mid-Tertiary unconformity west of the continental divide. Journal of Vertebrate Paleontology 27 (1), 204–224.

Biquand, D., Dubar, M., Sémah, F., 1990. Paleomagnetic correlation of the Mediterranean upper Neogene biochronology and Villafranchian vertebrate sites of the Massif central, France. Quaternary Research 33, 241–252.

Boehme, M., Abdul Aziz, H., Bachtadse, V., Prieto, J., Rocholl, A., Ulbig, A., Wijbrans, J.R., 2009. A new small-mammal biostratigraphy and high-resolution chronostratigraphic model for the Upper Freshwater Molasse of the eastern part of the North Alpine Foreland Basin (Bavaria, Germany). Geophysical Research Abstracts 11 EGU2009–0.

Botella, M., Vera, J.A., Porta, J., 1975. El yacimiento Achelense de la Solana de Zamborino. Fonelas. Granada (Primera campaña de excavaciones), 1. Cuadernos de Prehistoria de la Universidad de Granada, pp. 1–45.

Calvache, M.L., Viseras, C., Fernández, J., 1996. Evolution from endorheic to exorheic drainage in the Guadix Basin: geologic and geomorphic implications. In: Mather, A.E., Stokes, M. (Eds.), 2nd Cortijo Urra Field Meeting, SE Spain: Field Guide. University of Plymouth, pp. 43–48.

Calvache, M.L., Viseras, C., 1997. Long-term control mechanisms of stream piracy processes in southeast Spain. Earth Surface Processes and Landforms 22, 93–105.

Corvinus, G., Rimal, L.N., 2001. Biostratigraphy and geology of the Neogene Siwalik group of the Surai Khola and Rato Khola areas in Nepal. Palaeogeography, Palaeoclimatology, Palaeoecology 165, 251–279.

Dennell, R., Coard, R., Turner, A., 2006. The biostratigraphy and magnetic polarity zonation of the Pabbi Hills, northern Pakistan: an upper Siwalik (Pinjor stage) upper Pliocene–Lower Pleistocene fluvial sequence. Palaeogeography, Palaeoclimatology, Palaeoecology 234, 168–185.

Fernández, J., Bluck, B.J., Viseras, C., 1991. A lacustrine fan-delta system in the Pliocene deposits of the Guadix basin (Betic Cordilleras, South Spain). Cuadernos de Geología Ibérica 15, 299–317.

Fernández, J., Bluck, B.J., Viseras, C., 1993. The effects of fluctuating base level on the structure of alluvial fan and associated fan delta deposits: an example from the Tertiary of the Betic Cordillera, Spain. Sedimentology 40, 879–893.

Fernández, J., Soria, J.M., Viseras, C., 1996a. Stratigraphic architecture of the Neogene basins in the central sector of the Betic Cordillera (Spain): tectonic control and base level changes. In: Friend, P.F., Dabrio, C.J. (Eds.), Tertiary Basins of Spain: The Stratigraphic Record of Crustal Kinematics. Cambridge University Press, Cambridge, pp. 353–365.

Fernández, J., Viseras, C., Soria, J.M., 1996b. Pliocene–Pleistocene continental infilling of the Granada and Guadix basins (Betic Cordillera, Spain): the influence of allocyclic and autocyclic processes on the resultant stratigraphic organization. In: Friend, P.F., Dabrio, C.J. (Eds.), Tertiary Basins of Spain: The Stratigraphic Record of Crustal Kinematics. Cambridge University Press, Cambridge, pp. 366–371.

Garcés, M., Agustí, J., Parés, J.M., 1997. Late Pliocene continental magnetochronology in the Guadix-Baza basin (Betic ranges, Spain). Earth and Planetary Science Letters 146, 677–687.

García-Aguilar, J.M., 1997. La Cuenca de Guadix-Baza (Granada): evolución geodinámica y sedimentaria de los depósitos lacustres entre el Turoliense superior y el Pleistoceno. Ph.D. thesis (unpublished), University of Granada, 532 p.

García-Aguilar, J.M., Martín, J.M., 2000. Late Neogene to recent continental history and evolution of the Guadix-Baza basin (SE Spain). Revista de la Sociedad Geológica de España 13 (1), 65–77.

García-García, F., 2003. Modelos de sedimentación deltaica en las cuencas neógenas de la Cordillera Bética (sectores central y oriental). Ph.D. Thesis (unpublished), University of Granada, 333 p.

García-García, F., Fernández, J., Viseras, C., Soria, J.M., 2006a. Architecture and sedimentary facies evolution in a delta stack controlled by fault growth (Betic Cordillera, southern Spain, late Tortonian). Sedimentary Geology 185, 79–92.

García-García, F., Fernández, J., Viseras, C., Soria, J.M., 2006b. High frequency cyclicity in a vertical alternation of Gilbert-type deltas and carbonate bioconstructions in late the Tortonian, Tabernas Basin, Southern Spain. Sedimentary Geology 192, 123–139.

García-García, F., Soria, J.M., Viseras, C., Fernández, J., 2009. High frequence rhythmicity in a mixed siliciclastic - carbonate shelf (Late Miocene, Guadix basin, Spain). A model of interplay between climatic oscillations, subsidence and sediment dispersal. Journal of Sedimentary Research 79, 247–264.

Garrido, G. 2006. Paleontología sistemática de grandes mamíferos del yacimiento del Villafranquiense superior de Fonelas P-1 (Cuenca de Guadix, Granada). Ph.D. thesis (unpublished), University Complutense of Madrid, 726 p.

Garrido, G., Arribas, A., 2008. *Canis accitanus* nov. sp., a new small dog (Canidae, Carnivora, Mammalia) from the Fonelas P-1 Plio-Pleistocene site (Guadix basin, Granada, Spain). Geobios 41, 751–761.

Gibbard, P., Van Kolfschoten, T., 2004. The Pleistocene and Holocene epochs. In: Gradstein, F.M., Ogg, J.G., Smith, A.G. (Eds.), A Geological Time Scale 2004. Cambridge University Press, pp. 441–471.

Guérin, C., 1982. Première biozonation du Pléistocène européen, principal résultat biostratigraphique de l'étude des Rhinocerontidae (Mammalia, Perissodactyla) du Miocène terminal au Pléistocene supérieur d'Europe occidentale. Geobios 15 (4), 593–598.

Guérin, C., 1990. Biozones or mammal units? Methods and limits in biochronology. In: Lindsay, E.H., Fahlbusch, V., Mein, P. (Eds.), European Neogene Mammal Chronology. NATO ASI, Ser. A, vol. 180, pp. 119–130.

International Stratigraphic Chart IUGS, 2009. Available on-line in: http://www.stratigraphy.org.

Lindsay, E., 2001. Correlation of mammalian biochronology with the geomagnetic polarity time scale. Bolletino della Società Paleontologica Italiana 40 (2), 225–233.

Lourens, L., Hilgen, F.J., Shackleton, N.J., Laskar, J., Wilson, D., 2004. The Neogene period. In: Gradstein, F.M., Ogg, J.G., Smith, A.G. (Eds.), A Geological Time Scale 2004. Cambridge University Press, Cambridge, pp. 409–440.

MacFadden, B.J., Siles, O., Zeitler, P., Johnson, M.N., Campbell, K.E., 1983. Magnetic polarity stratigraphy of the middle Pleistocene (Ensenadan) Tarija formation of southern Bolivia. Quaternary Research 19, 172–187.

Miall, A.D., 1978. Lithofacies types and vertical profile models in braided rivers: a summary. In: Miall, A.D. (Ed.), Fluvial Sedimentology, 5. Canadian Society of Petroleum Geologists Memoirs, pp. 597–604.

Miall, A.D., 1985. Architectural-element analysis: a new method of facies analysis applied to fluvial deposits. Earth Science Reviews 22, 261–308.

Miall, A.D., 1996. The Geology of Fluvial Deposits. Sedimentary Facies, Basin Analysis and Petroleum Geology. Springer-Verlag, Berlin, 582 p.

Napoleone, G., Albianelli, A., Azzaroli, A., Mazzini, M., 2003. Dating the Villafranchian (Pliocene) vertebrate collections of the Upper Valdano (Tuscany, Italy) by the magnetochronologic framework of the basin fill. Bolletino della Società Paleontologica Italiana 42 (3), 301–313.

Oms, O., Dinarés-Turrel, J., Agustí, J., Parés, J.M., 1999. Refinements of the European mammal biochronology from the magnetic polarity record of the Plio–Pleistocene Zújar section, Guadix-Baza basin, SE Spain. Quaternary Research 51, 94–103.
Oms, O., Garcés, M., Parés, J.M., Agustí, J., Anadón, P., Juliá, R., 1994. Magnetostratigraphic characterization of a thick lower Pleistocene lacustrine sequence from Baza (Betic chain, Southern Spain). Physics of the Earth and Planetary Interiors 85, 173–180.
Opdyke, N., Mein, P., Lindsay, E., Pérez-Gonzales, A., Moissenet, E., Norton, V.L., 1997. Continental deposits, magnetostratigraphy and vertebrate paleontology, late Neogene of Eastern Spain. Palaeogeography, Palaeoclimatology, Palaeoecology 133, 129–148.
Peña, J.A., 1979. La Depresión de Guadix-Baza. Estratigrafía del Plio-Pleistoceno. PhD thesis (unpublished), University of Granada, 160 p.
Pla-Pueyo, S., 2009. Contexto estratigráfico y sedimentario de los yacimientos de grandes mamíferos del sector central de la Cuenca de Guadix (Cordilera Bética)./ Stratigraphic and sedimentary context of the large-mammal sites from the central sector of the Guadix Basin (Betic Cordillera). Ph.D. dissertation (unpublished), University of Granada, 287 p.
Pla-Pueyo, S., Gierlowski-Kordesch, E.H., Viseras, C., Soria, J.M., 2009a. Major controls on carbonate deposition during the evolution of a continental basin: Pliocene-Pleistocene of the Guadix Basin (Betic Cordillera, southern Spain). Sedimentary Geology 219, 97–114. doi:10.1016/j.sedgeo.2009.05.001.
Pla-Pueyo, S., Gierlowski-Kordesch, E.H., Viseras, C., Soria, J.M., 2009b. Sequence-stratigraphic model of a fluvio-lacustrine system in the Guadix Basin (Neogene, Betic Cordillera, Spain). 27th I.A.S. Meeting of Sedimentology, Alghero, Italy. Book of Abstracts, 316.
Pla-Pueyo, S., Viseras, C., García-García, F., Soria, J.M., 2009c. Sedimentology and paleoenvironmental interpretation of two calcareous tufas in the Guadix Basin (Betic Cordillera, Spain). 27th I.A.S. Meeting of Sedimentology, Alghero, Italy. Book of Abstracts, 643.
Pla-Pueyo, S., Yébenes, A., Viseras, C., Soria, J.M., Arribas, A., 2007. Palustrine sedimentation on a Pliocene-Pleistocene distal floodplain (Guadix Basin, Betic Cordillera, S. Spain). 25th I.A.S. Meeting of Sedimentology, Patras, Greece. Book of Abstracts, 140.
Scott, G.R., Gibert, L., 2009. The oldest hand-axes in Europe. Nature 461, 82–85.
Soria, J.M., 1993. La sedimentación neógena entre Sierra Arana y el río Guadiana Menor. Evolución desde un margen continental hasta una cuenca intramontañosa. Ph.D. Thesis, University of Granada, 292 pp.
Soria, J.M., Fernández, J., Viseras, C., 1999. Late Miocene stratigraphy and palaeogeographic evolution of the intramontane Guadix basin (Central Betic Cordillera, Spain): Implication for an Atlantic-Mediterranean connection. Palaeogeography, Palaeoclimatology, Palaeoecology 151, 255–266.
Soria, J.M., Viseras, C., Fernández, J., 1998. Late Miocene-Pleistocene tectono-sedimentary evolution and subsidence history of the central Betic Cordillera (Spain): a case study in the Guadix intramontane basin. Geological Magazine 135 (4), 565–574.
Tauxe, L., 2005. Inclination flattening and the geocentric axial dipole hypothesis. Earth and Planetary Science Letters 233, 247–261.
Viseras, C., 1991. Estratigrafía y sedimentología del relleno aluvial de la Cuenca de Guadix (Cordilleras Béticas). Ph.D. thesis, University of Granada, 327 pp.
Viseras, C., Fernández, J., 1992. Sedimentary basin destruction inferred from the evolution of drainage systems in the Betic Cordillera, southern Spain. Journal of the Geological Society (London) 149, 1021–1029.
Viseras, C., Fernández, J., 1994. Channel migration patterns and related sequences in some alluvial fan systems. Sedimentary Geology 88, 201–217.
Viseras, C., Fernández, J., 1995. The role of erosion and deposition in the construction of alluvial fan sequences in the Guadix Formation (SE Spain). Geologie en Mijnbouw 74, 21–33.
Viseras, C., Fernández, J., García-García, F., Soria, J.M., Calvache, M.L., Jáuregui, P., 2009. Dynamics of sedimentary environments in the accelerated siltation of a reservoir: the case of Alhama de Granada, southern Spain. Environmental Geology 56, 1353–1369. doi:10.1007/s00254-008-1231-2.
Viseras, C., Soria, J.M., Fernández, J., García García, F., 2005. The Neogene-Quaternary basins of the Betic Cordillera: an overview. Geophysical Research Abstracts 7, 11123–11127.
Viseras, C., Soria, J.M., Durán, J.J., Pla, S., Garrido, G., García-García, F., Arribas, A., 2006. A large-mammal site in a meandering fluvial context (Fonelas P-1, Late Pliocene, Guadix Basin, Spain). Sedimentological keys for its paleoenvironmental reconstruction. Palaeogeography, Palaeoclimatology, Palaeoecology 242, 139–168.
Wang, X., Qiu, Z., Li, Q., Wang, B., Qiu, Z., Downs, W.R., Xie, G., Xie, J., Deng, T., Takeuchi, G.T., Tseng, Z.J., Chang, M., Liu, J., Wang, Y., Biasatti, D., Sun, Z., Fang, X., Meng, Q., 2007. Vertebrate paleontology, biostratigraphy, geochronology, and paleoenvironment of Qaidam Basin in northern Tibetan Plateau. Palaeogeography, Palaeoclimatology, Palaeoecology 254, 363–385.
Whitelaw, M.J., 1992. Magnetic polarity stratigraphy of three Pliocene sections and inferences for the ages of vertebrate fossil sites near Bacchus Marsh, Victoria, Australia. Australian Journal of Earth Sciences 39, 521–528.
Web page of the Fonelas Project: http://www.igme.es/internet/museo/investigacion/paleontologia/fonelas/index.htm
Zijderveld, J.D.A., Hilgen, F.J., Langereis, C.G., Verhallen, P.J.J.M., Zachariasse, W.J., 1991. Integrated magnetostratigraphy and biostratigraphy of the upper Pliocene-lower Pleistocene from the Monte Singa and Crotone areas in Calabria, Italy. Earth and Planetary Science Letters 107, 697–714.